Prepared for submission to JHEP

FLAVOUR(267104)-ERC-93
CERN-PH-TH/2015-041

Anomalous triple gauge couplings from B-meson and kaon observables

Christoph Bobeth[1] **and Ulrich Haisch**[2,3]

[1] *Technische Universität München, Institute for Advanced Study, Lichtenbergstraße 2a, D-85748 Garching, Germany*

[2] *Rudolf Peierls Centre for Theoretical Physics, University of Oxford, OX1 3PN Oxford, United Kingdom*

[3] *CERN, Theory Division, CH-1211 Geneva 23, Switzerland*

E-mail: christoph.bobeth@ph.tum.de, u.haisch1@physics.ox.ac.uk

Abstract: We consider the three CP-conserving dimension-6 operators that encode the leading new-physics effects in the triple gauge couplings. The contributions to the standard-model electromagnetic dipole and semi-leptonic vector and axial-vector interactions that arise from the insertions of these operators are calculated. We show that radiative and rare B-meson decays provide, under certain assumptions, constraints on two out of the three anomalous couplings that are competitive with the restrictions obtained from LEP II, Tevatron and LHC data. The constraints arising from the $Z \to b\bar{b}$ electroweak pseudo observables, $K \to \pi\nu\bar{\nu}$ and ϵ'/ϵ are also studied.

Contents

1 Introduction

The tremendous experimental success of the standard model (SM) suggests that, at the weak scale, fundamental interactions respect a $SU(3)_C \times SU(2)_L \times U(1)_Y$ gauge symmetry and that any new state that may exist in nature is heavier than all known elementary particles. The discovery of a boson with a mass of 125 GeV and measurements of its production and decay rates at the LHC, give strong evidence for the Higgs mechanism, in which a linearly realised $SU(2)_L \times U(1)_Y$ symmetry is spontaneously broken to $U(1)_{\rm EM}$ by the Higgs vacuum expectation value. Weak-scale physics can therefore be described by an effective field theory (EFT) in which the SM Lagrangian is the leading term and new-physics effects are encoded in higher-dimensional operators constructed solely out of SM fields. Such an EFT description allows one to parametrise effects of heavy extra states in terms of operators with increasing dimension, which is equivalent to an expansion in inverse powers of a mass scale Λ that characterises the onset of new dynamics.

Constraints on the Wilson coefficients of the higher-dimensional operators come from electroweak (EW) precision observables. For instance, non-standard contributions to gauge boson two-point functions are severely constrained by oblique parameters as measured at the Z pole by LEP I [1]. Anomalous triple gauge couplings (TGCs) are bounded by measurements of gauge boson pair production performed at LEP II, the Tevatron and LHC (see e.g. [2–11]). Higgs-boson properties are also affected by the same higher-dimensional operators, which renders LHC measurements of the Higgs production and decay rates a powerful way to tighten the existing limits. Understanding the correlations between the different constraints and exploiting this knowledge to refine future new-physics searches will be an important task in the coming years.

In this article we extend the existing model-independent studies of the SM-EFT by deriving constraints on the CP-conserving TGCs using quark-flavour observables. While such restrictions have been studied previously [12–23], there are (at least) two good reasons that call for a new analysis. First, in the literature there exists no consensus on the analytic

form of the flavour-changing $\gamma d_i \bar{d}_j$ and $Z d_i \bar{d}_j$ one-loop vertices that result from the anomalous TGCs. By recalculating the one-loop contributions, we identify which of the available results are correct and which are not. Second, all earlier analyses are by now obsolete because they all predate the precision measurements of radiative and rare B-meson decays by BaBar, Belle and LHCb. Our study is based on the assumption that the TGCs are the only couplings that receive non-zero initial conditions at the scale Λ where new physics enters. This in particular means that we do neither allow for significant flavour-changing down-type interactions nor modifications of the $Zb\bar{b}$ couplings to occur at the new-physics scale Λ. Under this assumption, we show that radiative and rare B and K decays can provide constraints on two of the three TGCs that are comparable with the restrictions arising from high-energy observations. Like in case of anomalous $Zt\bar{t}$ couplings, this finding illustrates the complementarity and synergy between indirect [24] and direct [25] searches for physics beyond the SM.

The outline of this article is as follows. In Section 2 we discuss the three effective interactions to be examined in this paper and review how the SM-EFT operators are related to the TGC Lagrangian. The explicit calculations of the effects of anomalous TGCs in quark-flavour physics and in the $Z \to b\bar{b}$ pseudo observables are presented in Section 3. Our numerical analysis is performed in Section 4, while Section 5 contains our conclusions.

2 Preliminaries

The primary goal of our work is to derive indirect constraints on the following effective Lagrangian

$$\mathcal{L}_{\rm TGC} = \sum_{i=\phi B,\phi W,3W} \frac{C_i}{\Lambda^2}\, O_i\,, \tag{2.1}$$

which contains three C and P invariant dimension-6 operators that encode the leading effect of physics beyond the SM on the EW gauge boson self interactions. Here Λ is the new-physics scale at which the effective operators O_i are generated by integrating out heavy degrees of freedom. The Wilson coefficients C_i are hence understood to be evaluated at Λ. Like in [26], we write the operators in (2.1) as

$$\begin{aligned} O_{\phi B} &= (D_\mu \phi)^\dagger\, \hat{B}^{\mu\nu}\, (D_\nu \phi)\,, \\ O_{\phi W} &= (D_\mu \phi)^\dagger\, \hat{W}^{\mu\nu}\, (D_\nu \phi)\,, \\ O_{3W} &= \mathrm{Tr}\left(\hat{W}_{\mu\nu} \hat{W}^{\nu\rho} \hat{W}_\rho{}^\mu\right)\,, \end{aligned} \tag{2.2}$$

where $D_\mu \phi = \left(\partial_\mu + i g' B_\mu/2 + i g \sigma^a W^a_\mu/2\right) \phi$ is the covariant derivative acting on the Higgs doublet ϕ and σ^a are the usual Pauli matrices. The hatted field strength tensors are defined as $\hat{B}_{\mu\nu} = i g' \left(\partial_\mu B_\nu - \partial_\nu B_\mu\right)/2$ and $\hat{W}_{\mu\nu} = i g \sigma^a \left(\partial_\mu W^a_\nu - \partial_\nu W^a_\mu - g \epsilon_{abc} W^b_\mu W^c_\nu\right)/2$, while g' and g denotes the $U(1)_Y$ and $SU(2)_L$ gauge coupling, respectively.

The $SU(2)_L \times U(1)_Y$ gauge-invariant operators introduced in (2.2) modify the TGCs that we parametrise as ($V = \gamma, Z$) [27]

$$\mathcal{L}_{WWV} = -ig_{WWV}\left[g_1^V\left(W^+_{\mu\nu}W^{-\mu}V^\nu - W^+_\mu V_\nu W^{-\mu\nu}\right) + \kappa_V W^+_\mu W^-_\nu V^{\mu\nu} + \frac{\lambda_V}{m_W^2}W^+_{\mu\nu}W^{-\nu\rho}V_\rho{}^\mu\right]. \tag{2.3}$$

The overall coupling strengths are defined by $g_{WW\gamma} = gs_w = g'c_w = e$ and $g_{WWZ} = gc_w$ with s_w (c_w) denoting the sine (cosine) of the weak mixing angle, whereas $W^\pm_{\mu\nu} = \partial_\mu W^\pm_\nu - \partial_\nu W^\pm_\mu$ and $V_{\mu\nu} = \partial_\mu V_\nu - \partial_\nu V_\mu$ with $W^\pm_\mu$ and V_μ referring to the physical gauge boson fields.

Defining $g_1^V = 1 + \Delta g_1^V$ and $\kappa_V = 1 + \Delta\kappa_V$, the shifts Δg_1^V, $\Delta\kappa_V$ and the couplings λ_V can be identified with the Wilson coefficients C_i entering (2.1). Explicitly, the following simple relations are obtained [27]

$$\Delta g_1^Z = \frac{m_Z^2}{2\Lambda^2}C_{\phi W}\,, \qquad \Delta\kappa_\gamma = \frac{m_W^2}{2\Lambda^2}\left(C_{\phi B} + C_{\phi W}\right), \qquad \lambda_\gamma = \frac{3g^2m_W^2}{2\Lambda^2}C_{3W}\,, \tag{2.4}$$

with m_W (m_Z) denoting the mass of the W (Z) boson. Furthermore, one has $\Delta g_1^\gamma = 0$ as a result of gauge invariance and[1]

$$\Delta\kappa_Z = \Delta g_1^Z - \frac{s_w^2}{c_w^2}\Delta\kappa_\gamma\,, \qquad \lambda_Z = \lambda_\gamma\,. \tag{2.5}$$

It follows that only three of the five non-zero anomalous TGCs are linearly independent. Hereafter we choose these three independent parameters to be Δg_1^Z, $\Delta\kappa_\gamma$ and λ_γ.

It is important to realise that the effective Lagrangian introduced in (2.1) provides only a small subset of the dimension-6 operators of the full SM-EFT Lagrangian (cf. [28, 29]). In order to derive bounds on the anomalous TGCs (2.4), we make in the following the assumption that the Wilson coefficients of all the (relevant) SM-EFT operators but $C_{\phi B}$, $C_{\phi W}$ and C_{3W} vanish at the scale Λ. Notice furthermore that the operator O_{3W} can only be generated at the loop level in any model of new physics, while $O_{\phi B}$ and $O_{\phi W}$ can receive corrections at tree level. The coefficient λ_γ is thus expected to be suppressed compared to Δg_1^Z and $\Delta\kappa_\gamma$ in a large class of scenarios of physics beyond the SM.

3 Analytic results

The Lagrangian introduced in (2.3) gives rise to contributions to radiative and rare B decays, kaon physics and the $Z \to b\bar{b}$ decay. In this section, we calculate the leading TGC corrections to the phenomenologically most relevant of these observables. The computation proceeds in two steps. First, renormalisation group (RG) evolution of the Wilson coefficients of the SM-EFT operators from the new-physics scale Λ down to the weak scale of order m_W. This step depends crucially on the choice of initial conditions, and we assume that only

[1] These two relations are only valid if the analysis is limited to dimension-6 operators [26]. For new-physics scales Λ sufficiently above the weak scale, dimension-8 terms are however small, rendering them phenomenologically irrelevant at present.

the TGC operators $O_{\phi B}$, $O_{\phi W}$ and O_{3W} receive non-zero Wilson coefficients at Λ. Second, calculation of matching corrections to the Fermi theory at the weak scale obtained by integrating out the top quark as well as the Higgs, Z and W boson.

In the case of the $b \to s\gamma, \ell^+\ell^-$ observables, one determines in this way the corrections ΔC_i to the Wilson coefficients $C_i = (C_i)_{\rm SM} + \Delta C_i$ of the operators that enter the effective Lagrangian of $|\Delta B| = |\Delta S| = 1$ decays

$$\mathcal{L}_{|\Delta B|=|\Delta S|=1} = \frac{4G_F}{\sqrt{2}} V_{ts}^* V_{tb} \left(C_7 Q_7 + C_9 Q_9 + C_{10} Q_{10} \right) + \text{h.c.} \tag{3.1}$$

Here and below the $|\Delta B| = |\Delta S| = 1$ Wilson coefficients C_i as well as ΔC_i $(i = 7, 9, 10)$ are understood to be evaluated at m_W, the Fermi constant is denoted by G_F and V_{ij} are the elements of the Cabibbo-Kobayashi-Maskawa matrix. The electromagnetic dipole, semi-leptonic vector and axial-vector operators are defined as

$$\begin{aligned} Q_7 &= \frac{e}{(4\pi)^2} m_b \left(\bar{s}_L \sigma_{\alpha\beta} b_R \right) F^{\alpha\beta} , \\ Q_9 &= \frac{e^2}{(4\pi)^2} \left(\bar{s}_L \gamma_\alpha b_L \right) \left(\bar{\ell} \gamma^\alpha \ell \right) , \\ Q_{10} &= \frac{e^2}{(4\pi)^2} \left(\bar{s}_L \gamma_\alpha b_L \right) \left(\bar{\ell} \gamma^\alpha \gamma_5 \ell \right) , \end{aligned} \tag{3.2}$$

with L, R indicating the chirality of the fermionic fields, $\sigma_{\alpha\beta} = i \left[\gamma_\alpha, \gamma_\beta \right] / 2$ and $F_{\alpha\beta}$ the field strength tensor of QED. The effective Lagrangians for $b \to d$ and $s \to d$ transitions are found from (3.1) and (3.2) by appropriate replacements. The current-current and QCD penguin operators are not affected by the TGCs at the one-loop level.

The Feynman graphs that give rise to the modifications ΔC_7, ΔC_9 and ΔC_{10} are depicted in Figure 1. In terms of the three parameters Δg_1^Z, $\Delta\kappa_\gamma$ and λ_γ (see (2.4)), we arrive at

$$\begin{aligned} \Delta C_7 &= \Delta\kappa_\gamma f_7^\kappa(x_t) + \lambda_\gamma f_7^\lambda(x_t) , \\ \Delta C_9 &= -\Delta D + \lambda_\gamma f_9^\lambda(x_t) + \frac{1 - 4s_w^2}{s_w^2} \Delta C , \\ \Delta C_{10} &= -\frac{1}{s_w^2} \Delta C , \end{aligned} \tag{3.3}$$

with $x_t = m_t^2 / m_W^2$ and

$$\begin{aligned} f_7^\kappa(x) &= -\frac{x}{2(x-1)^2} - \frac{x^3 - 3x^2}{4(x-1)^3} \ln x , \\ f_7^\lambda(x) &= \frac{x^2 + x}{4(x-1)^2} - \frac{x^2}{2(x-1)^3} \ln x , \\ f_9^\lambda(x) &= -\frac{3x^2 - x}{2(x-1)^2} + \frac{x^3}{(x-1)^3} \ln x . \end{aligned} \tag{3.4}$$

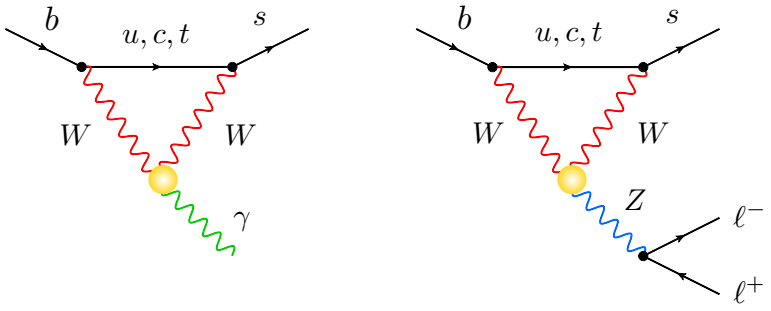

Figure 1. Examples of one-loop diagrams that generate a $b \to s\gamma$ (left) and a $b \to s\ell^+\ell^-$ (right) transition. The insertions of the TGC operators are indicated by yellow circles, while the SM vertices are represented by black dots.

For the universal Z-penguin (photon-penguin) coefficient ΔC (ΔD) entering both ΔC_9 and ΔC_{10} (ΔC_9), we obtain

$$\Delta C = \frac{3c_w^2}{8}\,\Delta g_1^Z\,x_t\,\ln\left(\frac{\Lambda^2}{m_W^2}\right)\,, \qquad \Delta D = \frac{1}{4}\,\Delta\kappa_\gamma\,x_t\,\ln\left(\frac{\Lambda^2}{m_W^2}\right)\,. \tag{3.5}$$

Our analytic result for ΔC_7 as given in (4.8) agrees with the expression that derives from the calculations [12, 14, 19]. It however differs from the findings reported in [13, 15, 22]. In the case of ΔC_9 and ΔC_{10}, the given expressions can be obtained by combining the results of [13, 16, 17, 23]. On the other hand, our result for the term in ΔC_9 proportional to $\Delta\kappa_\gamma$ does not agree with [12], while it differs by a sign from [20].

The Inami-Lim functions (3.4) and (3.5) can be divided into two categories. First, the large logarithms in (3.5) encode the leading-logarithmic (LL) contributions associated to the RG evolution between Λ and m_W. We have verified that the coefficients of these $\ln\left(\Lambda^2/m_W^2\right)$ terms can be recovered from the anomalous dimensions given in [30]. This provides a non-trivial cross-check since the latter calculation is performed in a different operator basis [28, 29]. It furthermore shows that the corresponding ultraviolet (UV) divergences are properly absorbed into counterterms in the context of the complete operator basis of the SM-EFT. Notice that a resummation of LL effects is possible, but given that $y_t^2/(4\pi)^2\,\ln\left(\Lambda^2/m_W^2\right) \ll 1$ with y_t the top-quark Yukawa coupling, keeping the $\ln\left(\Lambda^2/m_W^2\right)$ terms unresummed is a good approximation. A second type of contributions to the coefficients ΔC_i comes from the evaluation of the matrix elements of the TGC operators at the scale m_W. The corrections of this sort are encoded in the Inami-Lim functions (3.4) and do not contain $\ln\left(\Lambda^2/m_W^2\right)$ terms. They constitute the leading effects of $\Delta\kappa_\gamma$ in C_7 and λ_γ in C_7 and C_9. On the other hand, finite matching corrections are not included in the case of the LL universal terms (see for instance [31, 32] for related discussions) since they are formally subleading, i.e. of next-to-leading logarithmic order (NLL). Incorporating such NLL effects might however be mandatory in future precision studies.

We finally observe that the functions $f_7^\kappa(x)$ and $f_7^\lambda(x)$ in (3.4) scale as x for $x \ll 1$. This implies that the TGC corrections to the anomalous magnetic moment of the muon a_μ are proportional to $\sum_{i=1}^3 |U_{\mu i}|^2\,m_{\nu_i}^2/m_W^2$ with $U_{\mu i}$ denoting the elements of the Pontecorvo-

Maki-Nakagawa-Sakata mixing matrix. Due to the strong chiral suppression by the neutrino masses, the TGC contributions to a_μ are unobservably small. The same statements apply to lepton-flavour violating decays like $\mu \to e\gamma$ and $\mu \to 3e$.

The coefficient ΔC also contributes to the rare $K \to \pi\nu\bar{\nu}$ decays, while both ΔC and ΔD affect the observable ϵ'/ϵ, which measure the amount of direct CP violation in the $K \to \pi\pi$ system. It is well-known (see e.g. Section III.2.2 of [33]) that these observables are very sensitive probes of modifications in the EW penguin sector, and we will give the relevant formulas that allow for a phenomenological analysis in the next section.

In the presence of (2.4) the interactions between the Z boson and bottom quarks are modified at the one-loop level as well. We parameterise the resulting effective $Zb\bar{b}$ couplings at the weak scale as follows

$$\mathcal{L}_{Zb\bar{b}} = \frac{e}{s_w c_w}\left[\left(g_L^b + \delta g_L^b\right)\bar{b}_L \not{Z} b_L + g_R^b\,\bar{b}_R \not{Z} b_R\right], \tag{3.6}$$

with $g_L^b = -1/2 + s_w^2/3$ and $g_R^b = s_w^2/3$. For the one-loop correction δg_L^b associated to the anomalous TGCs, we obtain the compact expression

$$\delta g_L^b = \frac{\alpha}{2\pi s_w^2}\,|V_{tb}|^2\left(\Delta C + \delta C\right), \tag{3.7}$$

where ΔC can be found in (3.5) and

$$\delta C = \frac{1}{16}\,\Delta\kappa_Z\, x_t\, \ln\left(\frac{\Lambda^2}{m_W^2}\right), \tag{3.8}$$

with $\Delta\kappa_Z$ given in (2.5). Note that the correction δC in (3.7) arises from expanding the $Z \to b\bar{b}$ amplitude to second order with respect to the external momenta (cf. [34, 35]). At the Z pole these effects scale as m_Z^2/m_W^2 with respect to ΔC, while in B-meson (kaon) decays they are of order m_b^2/m_W^2 (m_c^2/m_W^2), and thus can be safely neglected. Like in the case of ΔD and ΔC, we have included in δC only the LL effects. Our results (3.7) and (3.8) agree with the expressions given in [21].

4 Numerical analysis

In this section we analyse the constraints on Δg_1^Z, $\Delta\kappa_\gamma$ and λ_γ that arise from indirect probes. We start our discussion by considering the inclusive radiative B-meson decay. In terms of the shift ΔC_7, the ratio between the new-physics branching ratio of $B \to X_s\gamma$ and the SM prediction can be written as [36]

$$R_{X_s} = \frac{\mathrm{Br}\left(B \to X_s\gamma\right)}{\mathrm{Br}\left(B \to X_s\gamma\right)_{\mathrm{SM}}} = 1 - 2.45\,\Delta C_7\,. \tag{4.1}$$

Combining the latest SM calculation [36, 37] with the present world average [38], one gets

$$R_{X_s} = 1.02 \pm 0.10\,, \tag{4.2}$$

if uncertainties are added in quadrature.

In the case of the $B_s \to \mu^+\mu^-$ decay, we arrive instead at the simple formula

$$R_{\mu^+\mu^-} = \frac{\text{Br}\,(B_s \to \mu^+\mu^-)}{\text{Br}\,(B_s \to \mu^+\mu^-)_{\text{SM}}} = \left(1 - 0.25\,\Delta C_{10}\right)^2 . \tag{4.3}$$

To constrain the coefficient ΔC_{10}, this result should be compared to

$$R_{\mu^+\mu^-} = 0.78 \pm 0.18\,, \tag{4.4}$$

which we have obtained from the recently improved SM prediction [39–41] and the combined CMS and LHCb result [42] by treating the individual uncertainties as Gaussian errors.

In order to set bounds on the TGCs from the modified $Zb\bar{b}$ couplings (3.6), we employ the result of a recent global analysis of EW precision observables [43], which reads

$$\delta g_L^b = 0.0016 \pm 0.0015\,. \tag{4.5}$$

It is important to realise that the SM predictions for $\text{Br}\,(B \to X_s\gamma)$, $\text{Br}\,(B_s \to \mu^+\mu^-)$ and $\Gamma\left(Z \to b\bar{b}\right)$ are all under good control, having theoretical uncertainties below the 10% level. Combining the three constraints R_{X_s}, $R_{\mu^+\mu^-}$ and δg_L^b therefore allows for a clean extraction of the TGC parameters Δg_1^Z, $\Delta\kappa_\gamma$ and λ_γ. The resulting constraints on the different pairs of coefficients are shown in the three panels of Figure 2. The yellow and orange contours represent the 68% confidence level (CL) ($\Delta\chi^2 = \chi^2 - \chi^2_{\text{SM}} = 2.3$ with $\chi^2_{\text{SM}} = 2.6$) and 95% CL ($\Delta\chi^2 = 6.0$) regions arising from the global fit, while the coloured bands correspond to the 68% CL regions following from the individual constraints. The parameter not depicted in each panel has been set to zero and the new-physics scale Λ appearing in (3.5) and (3.8) has been fixed to 2 TeV. This choice of Λ will be employed throughout our article. Slightly weaker restrictions would be obtained for lower values of Λ. From the panels it is evident that the most tightly constrained TGC is Δg_1^Z, and that these bounds are driven by (4.4). This feature is readily understood by noticing that the relevant Wilson coefficient scales as $\Delta C_{10} \sim -\Delta g_1^Z\, x_t \ln\left(\Lambda^2/m_W^2\right)$, whereas one has $\Delta C_7 \sim -\Delta\kappa_\gamma \ln x_t$ in the limit $x_t \to \infty$ of infinitely heavy top quark. Explicitly, we find in the case $\lambda_\gamma = 0$ (upper left panel) the following 68% CL constraints

$$\Delta g_1^Z = -0.009 \pm 0.019\,, \qquad \Delta\kappa_\gamma = 0.00 \pm 0.16\,, \tag{4.6}$$

and the correlation matrix

$$\rho = \begin{pmatrix} 1 & -0.06 \\ -0.06 & 1 \end{pmatrix} . \tag{4.7}$$

The above numbers should be contrasted with the limits that can be derived from EW gauge boson pair production at LEP II, the Tevatron and the LHC as well as Higgs physics (see e.g. [2–11]). For instance, assuming $|\lambda_\gamma| \ll \left|\Delta g_1^Z\right|, |\Delta\kappa_\gamma|$, the recent analysis [11] of the $e^+e^- \to W^+W^-$ production data collected by the LEP II experiments obtains the model-independent 68% CL bounds $\Delta g_1^Z = -0.06 \pm 0.03$ and $\Delta\kappa_\gamma = 0.06 \pm 0.04$. We see that compared to (4.6) the LEP II limit on Δg_1^Z is slightly weaker, while in the case of the parameter $\Delta\kappa_\gamma$ the LEP II constraint is clearly superior. The strong sensitivity of

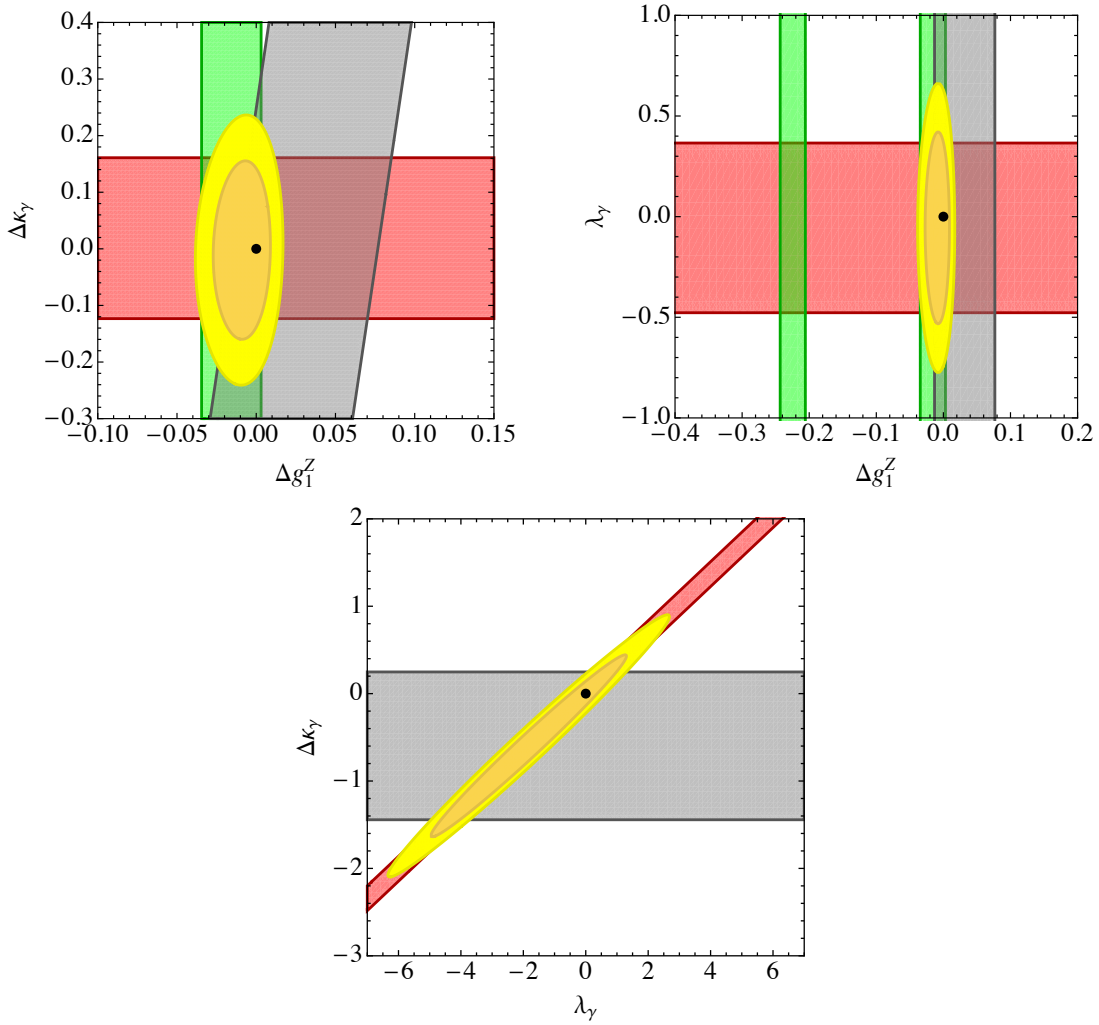

Figure 2. Allowed regions in the Δg_1^Z–$\Delta\kappa_\gamma$ plane (upper left panel), the Δg_1^Z–λ_γ plane (upper right panel) and the λ_γ–$\Delta\kappa_\gamma$ plane (lower panel). The red, green and grey contours correspond to the 68% CL best fit regions following from $B \to X_s\gamma$, $B_s \to \mu^+\mu^-$ and $Z \to b\bar{b}$, respectively. The yellow and orange contours show the 68% CL and 95% CL regions arising from a combination of the individual constraints. The shown constraints have been obtained for $\Lambda = 2\,\text{TeV}$. The black points correspond to the SM.

$B_s \to \mu^+\mu^-$ to the TGC Δg_1^Z nicely illustrates the role of this decay mode as an EW precision test [44].

From the upper right and lower panel in Figure 2 one observes in addition that the constraints on λ_γ are notably less stringent than those on Δg_1^Z and $\Delta\kappa_\gamma$. The reason for this is twofold. First, only $B \to X_s\gamma$ is sensitive to λ_γ and the contribution is not logarithmically enhanced, scaling like $\Delta C_7 \sim \lambda_\gamma$. Second, the R_{X_s} constraint (4.1) has an approximately blind direction along $\Delta\kappa_\gamma \simeq 1/3\,\lambda_\gamma$. In consequence, our bounds on λ_γ are not competitive with those that derive for instance from EW gauge boson production at LEP II, which read $\lambda_\gamma = 0.00 \pm 0.07$ [11]. Observe that the $R_{\mu^+\mu^-}$ constraint allows in

principle for large destructive new-physics contributions that would effectively flip the sign of the $B_s \to \mu^+\mu^-$ amplitude. This feature is illustrated by the second green band in the upper right panel. One also sees that the corresponding ambiguity in Δg_1^Z is resolved by $Z \to b\bar{b}$. In the case of $B \to X_s\gamma$ a similar ambiguity exists, but it is not shown in the lower panel, because the existing informations on $b \to s\ell^+\ell^-$ transitions can be used to eliminate this possibility [45].[2]

The quark-flavour observables (4.1) and (4.3) that we have considered so far are only sensitive to the shifts ΔC_7 and ΔC_{10}, but are unaffected by a possible new-physics contribution ΔC_9. In order to gain sensitivity to ΔC_9 one has to include informations on the $b \to s\ell^+\ell^-$ transitions in the global fit. The recent analysis [47] is based on 78 independent measurements of radiative and rare $b \to s$ observables. It finds the constraints

$$\Delta C_7 = -0.03 \pm 0.03\,, \qquad \Delta C_9 = -1.17 \pm 0.40\,, \qquad \Delta C_{10} = 0.12 \pm 0.27\,, \tag{4.8}$$

at 68% CL and the correlations

$$\rho = \begin{pmatrix} 1 & -0.22 & 0.02 \\ -0.22 & 1 & 0.31 \\ 0.02 & 0.31 & 1 \end{pmatrix}. \tag{4.9}$$

The corresponding χ^2 in the SM is 104.6, while the best-fit point of the new-physics hypothesis has a χ^2 of 90.6. Note that (4.8) correspond to a tension between the SM predictions and the data at the level of 3σ. While further LHCb studies of $B \to K^*\mu^+\mu^-$, $B^+ \to K^+\mu^+\mu^-$ and $B_s \to \phi\mu^+\mu^-$ and a better understanding of hadronic uncertainties will be necessary to clarify whether the observed deviation is a real sign of new physics, we will combine (4.8) with (4.5) to set bounds on the TGC parameters. This exercise will illustrate the power of modes like $B \to K^*\mu^+\mu^-$ in constraining the values of Δg_1^Z, $\Delta\kappa_\gamma$ and λ_γ. Of course the final results of our analysis should be taken with a pinch of salt, because the anomalies in the $b \to s\ell^+\ell^-$ sector may become smaller (or even disappear) once LHCb has analysed the full LHC run-1 data set.

By building a $\Delta\chi^2$ from (4.5) and (4.8), we obtain the allowed 68% CL ($\Delta\chi^2 = 2.3$) and 95% CL ($\Delta\chi^2 = 6.0$) regions in the Δg_1^Z–$\Delta\kappa_\gamma$, Δg_1^Z–λ_γ and λ_γ–$\Delta\kappa_\gamma$ planes shown in Figure 3. For $\lambda_\gamma = 0$ (upper left panel), we obtain the 68% CL constraints

$$\Delta g_1^Z = -0.003 \pm 0.007\,, \qquad \Delta\kappa_\gamma = 0.13 \pm 0.04\,, \tag{4.10}$$

with the correlations

$$\rho = \begin{pmatrix} 1 & -0.32 \\ -0.32 & 1 \end{pmatrix}. \tag{4.11}$$

Comparing the numbers in (4.10) with those quoted in (4.6), one sees that including the information on the inclusive and exclusive $b \to s\ell^+\ell^-$ transitions improves the constraints that can be put on the TGC parameter $\Delta\kappa_\gamma$ notably. In fact, the uncertainty on $\Delta\kappa_\gamma$ is

[2] The latest model-independent fit that allows for all solutions finds a strong posterior preference for the SM-like sign solution of C_7, C_9 and C_{10} of 4 to 1 compared to the sign-flipped case [46].

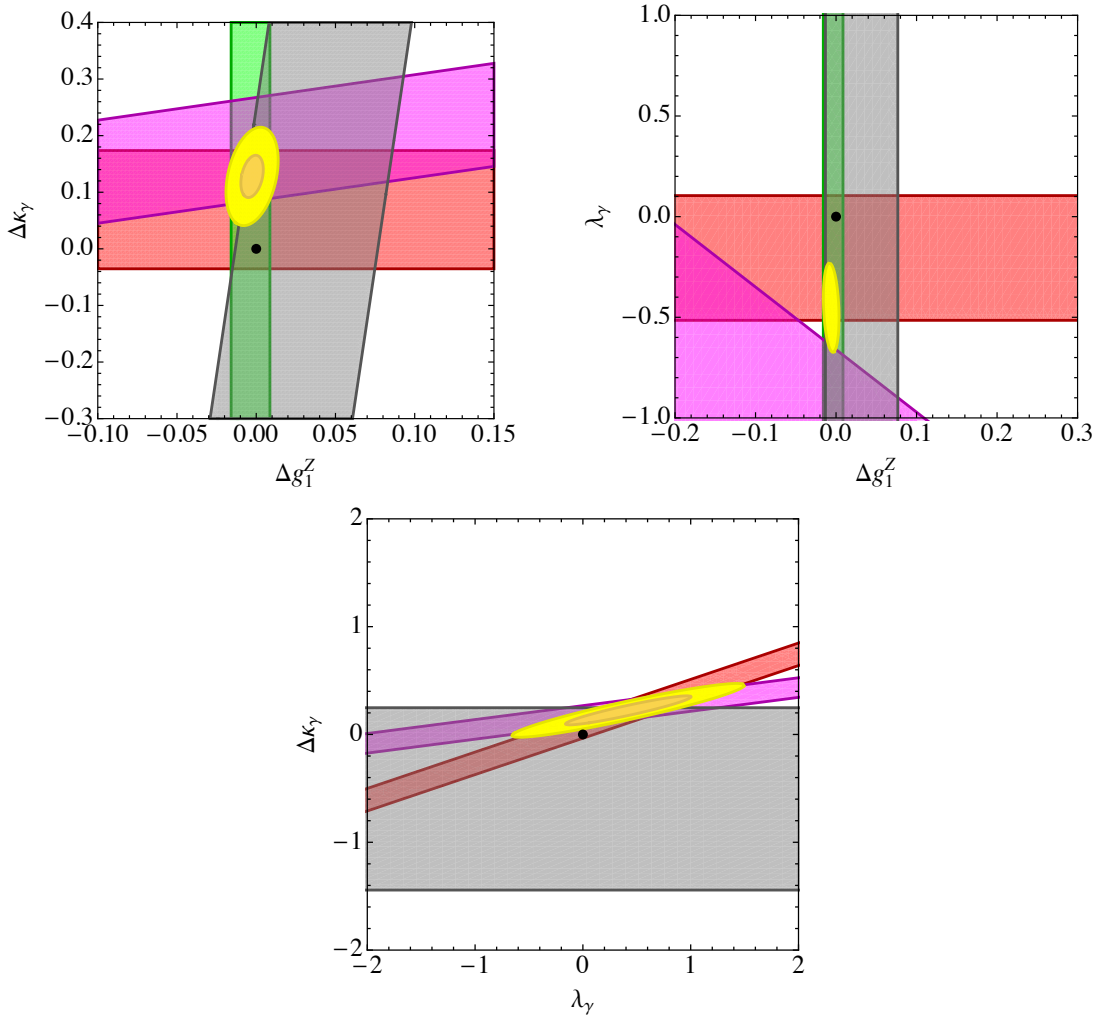

Figure 3. Allowed regions in the Δg_1^Z–$\Delta\kappa_\gamma$ plane (upper left panel), the Δg_1^Z–λ_γ plane (upper right panel) and the λ_γ–$\Delta\kappa_\gamma$ plane (lower panel). The red, magenta, green and grey contours correspond to the 68% CL best fit regions following from ΔC_7, ΔC_9, ΔC_{10} and δg_L^b, respectively. The dominant constraint on ΔC_7 arises from $B \to X_s\gamma$, while ΔC_9 is bounded most strongly by $B \to K^*\mu^+\mu^-$. The constraint ΔC_{10} is driven by the combination of $B \to K^{(*)}\mu^+\mu^-$, $B_s \to \phi\mu^+\mu^-$ and $B_s \to \mu^+\mu^-$. The yellow and orange contours show the 68% CL and 95% CL regions arising from a combination of the individual constraints. All constraints employ $\Lambda = 2\,\text{TeV}$. The black points correspond to the SM.

now comparable to the one found in [11] from a study of W^+W^- production at LEP II. Our findings illustrate that precision measurements of $B \to K^{(*)}\mu^+\mu^-$ and $B_s \to \phi\mu^+\mu^-$, possible at LHCb, provide yet another powerful probe of EW physics. Notice also that the best fit point in (4.10) corresponds to a large destructive photon penguin with $\Delta D \simeq 1$. Such a photon penguin has to arise from a strongly-coupled theory with new states not far above the weak scale that predicts in addition $|C_{\phi B}| \gg |C_{\phi W}|$ and $C_{\phi B} > 0$. While it seems challenging to construct a viable UV completion with these features, the possibility that an anomalous photon penguin explains (part of) the deviations seen in semi-leptonic

$b \to s$ transitions cannot be excluded in a model-independent fashion.[3]

From the upper right panel, one furthermore observes that in scenarios with $\Delta\kappa_\gamma = 0$ one cannot obtain the results (4.10) within the 68% CL. This feature is easy to understand by noting that the parameter Δg_1^Z enters ΔC_9 relative to ΔC_{10} with a factor of $-1+4s_w^2 \simeq -0.08$. A large Z-penguin contribution ΔC that gives rise to $\Delta C_9 = \mathcal{O}(-1)$ thus implies $\Delta C_{10} = \mathcal{O}(10)$, which is clearly incompatible with data. The lower panel finally illustrates that including $b \to s\ell^+\ell^-$ transitions in the global fit helps to partly lift the blind direction along $\Delta\kappa_\gamma \simeq 1/3\,\lambda_\gamma$, because these modes depend on ΔC_7 and ΔC_9, which both are sensitive to λ_γ. Still the existing quark-flavour data is unable to probe values $|\lambda_\gamma| \lesssim \mathcal{O}(1)$, which implies, that compared to other collider probes, radiative and rare $b \to s$ modes do not add any relevant information on the latter TGC parameter.

Future precision measurements of the rare $K \to \pi\nu\bar\nu$ decays have the potential to further improve the constraints on the TGC Δg_1^Z. Employing the results of [49–52], we obtain

$$\begin{aligned} R_{K^+} &= \frac{\text{Br}\,(K^+ \to \pi^+\nu\bar\nu)}{\text{Br}\,(K^+ \to \pi^+\nu\bar\nu)_{\text{SM}}} = 1 + 0.93\Delta C + 0.22\,(\Delta C)^2\,, \\ R_{K^0} &= \frac{\text{Br}\,\big(K_L^0 \to \pi^0\nu\bar\nu\big)}{\text{Br}\,\big(K_L^0 \to \pi^0\nu\bar\nu\big)_{\text{SM}}} = 1 + 1.36\Delta C + 0.46\,(\Delta C)^2\,. \end{aligned} \tag{4.12}$$

Using these formulas together with (3.5) allows one to translate two-sided limits on Δg_1^Z into allowed ranges for R_{K^+} and R_{K^0}. From (4.6), one finds for example

$$R_{K^+} = [0.81, 1.07]\,, \qquad R_{K^0} = [0.73, 1.10]\,. \tag{4.13}$$

These numbers should be compared to the sensitivity that the NA62 [53] and KOTO [54] experiments plan to achieve. The NA62 goal is a measurement of the $K^+ \to \pi^+\nu\bar\nu$ branching ratio with 10% precision, which starts to test the R_{K^+} range quoted in (4.13). In contrast, achieving SM sensitivity to the $K_L^0 \to \pi^0\nu\bar\nu$ branching ratio as anticipated by KOTO is not sufficient to probe the size of the corrections in R_{K^0} that can arise from the presently allowed shifts Δg_1^Z. In order to notably improve the constraints on the TGC Δg_1^Z, measurements of the $K \to \pi\nu\bar\nu$ branching ratios at the level of a few percent thus seem to be needed. In the case of $K^+ \to \pi^+\nu\bar\nu$, the proposed ORKA experiment [55] may provide such an accuracy.

Another kaon observable that can provide powerful probes of the EW penguin sector is the ratio ϵ'/ϵ. Including new-physics effects from both the Z-boson and the photon, this quantity can be calculated from (see e.g. [56, 57])

$$\frac{\epsilon'}{\epsilon} = \Big(-2.3 + 21.0\,R_6 - 8.0\,R_8 + \Big[(1.2 + 0.2R_6)\,\Delta C + (0.9 - 16.2\,R_8)\,\Delta Z\Big]\Big)\cdot 10^{-4}\,. \tag{4.14}$$

Here R_6 as well as R_8 denote hadronic parameters and

$$\Delta Z = \Delta C + \frac{1}{4}\Big(\Delta D - \lambda_\gamma\, f_9^\lambda(x_t)\Big)\,. \tag{4.15}$$

[3] Needless to say that a photon penguin is unable to address the anomaly observed recently by LHCb in the ratio R_K of $B^+ \to K^+\mu^+\mu^-$ and $B^+ \to K^+e^+e^-$ branching ratios at low di-lepton invariant mass [48].

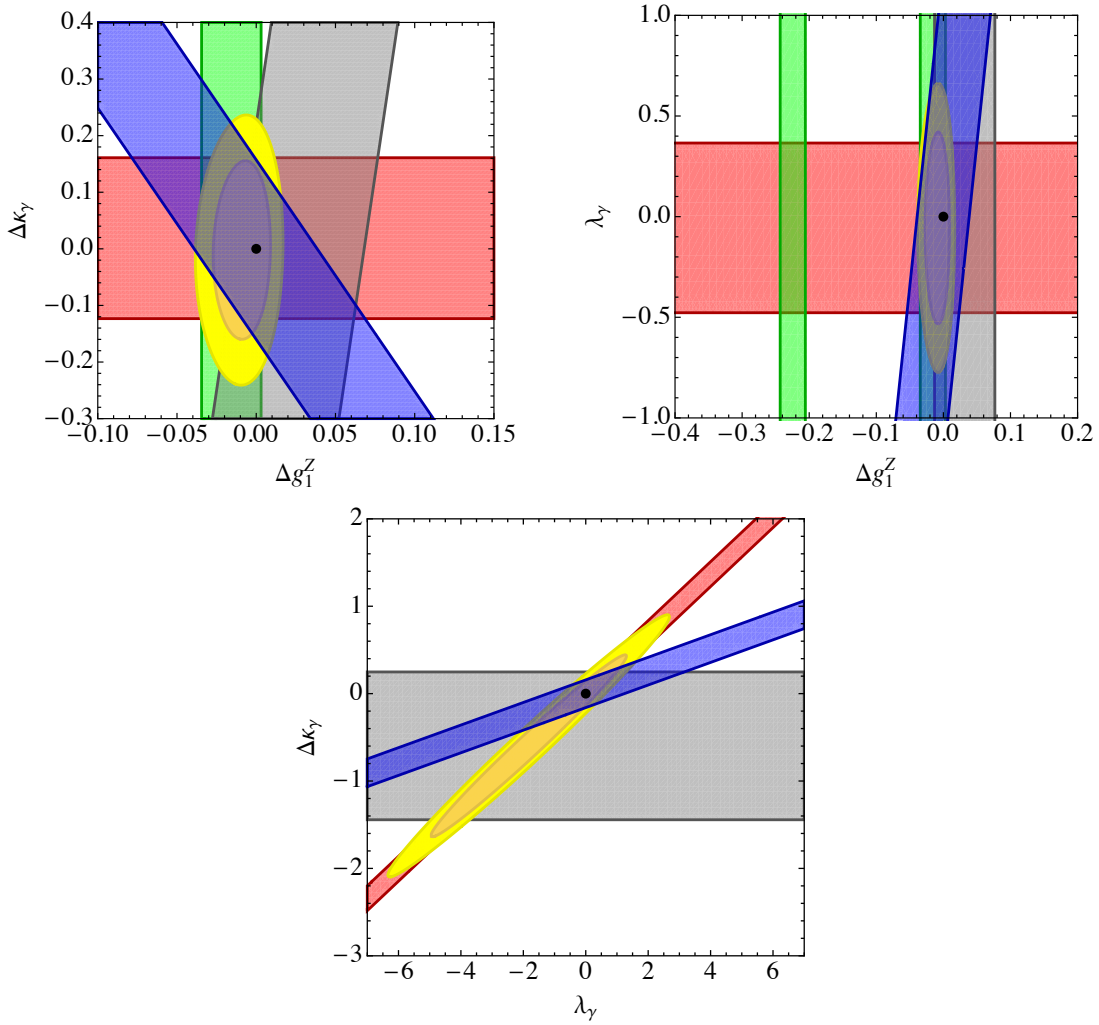

Figure 4. The blue contours indicate possible future 68% CL constraints in the Δg_1^Z–$\Delta\kappa_\gamma$ plane (upper left panel), the Δg_1^Z–λ_γ plane (upper right panel) and the λ_γ–$\Delta\kappa_\gamma$ plane (lower panel) arising from a future SM calculation of ϵ'/ϵ with an assumed total theoretical uncertainty of 20%. The remaining constraints are those shown in Figure 2. All restrictions use $\Lambda = 2\,\text{TeV}$.

To obtain useful constraints from (4.14), the quantities R_6 and R_8 have to be known with sufficient precision. While there is at present no reliable result for R_6, lattice QCD calculations of R_8 have matured in recent years [58] and provide the value $R_8 \simeq 0.83$ [59]. Anticipating further progress in the lattice QCD calculations of the hadronic parameters R_6 and R_8, a full SM calculation of ϵ'/ϵ with a total uncertainty of 20% may be possible in the near future (see Section X.3.2.1 of [33]).

The blue contours in Figure 4 illustrate the impact that a SM calculation of ϵ'/ϵ with a total error of 20% could have in constraining the TGC parameters Δg_1^Z and $\Delta\kappa_\gamma$. To obtain the shown 68% CL ($\Delta\chi^2 = 2.3$) bounds, we have chosen $R_6 = 1.21$ and $R_8 = 0.83$. With this input our SM prediction reproduces the central value of the experimental determination $\epsilon'/\epsilon = (16.5 \pm 2.6) \cdot 10^{-4}$ [60]. From all three panels one observes that with a theoretical

precision of 20%, the ratio ϵ'/ϵ will start to provide additional meaningful constraints on the TGCs. Our formula (4.14) together with (3.4) and (3.5) allows to monitor the effect that any theoretical improvement concerning the calculation of the hadronic parameters R_6 and R_8 will have on the extraction of Δg_1^Z, $\Delta\kappa_\gamma$ and λ_γ from direct CP violation in the $K \to \pi\pi$ system.

5 Conclusions

In this paper we have calculated the one-loop corrections to the flavour-changing electromagnetic dipole and semi-leptonic vector and axial-vector interactions that arise from Feynman diagrams involving anomalous CP-conserving TGCs. Although such computations have been performed before by various groups, another independent calculation was necessary because the analytic results given in the literature differ between publications. With the help of our explicit computation we are able to identify the correct one-loop results and collect them here for the first time.

Employing our analytic results, we have performed a model-independent EFT study of the constraints on the three TGC parameters Δg_1^Z, $\Delta\kappa_\gamma$ and λ_γ using low-energy measurements. Our analysis is based on the assumption that the TGC operators are the only SM-EFT interactions that receive non-zero initial conditions at the new-physics scale Λ. The magnitude of Δg_1^Z, $\Delta\kappa_\gamma$ and λ_γ is then determined from a comparison with the present experimental data on $B \to X_s\gamma$, $B_s \to \mu^+\mu^-$, $B \to X_s\ell^+\ell^-$, $B \to K^{(*)}\mu^+\mu^-$, $B_s \to \phi\mu^+\mu^-$ and $Z \to b\bar{b}$. We find that while the constraints on the two parameters Δg_1^Z and $\Delta\kappa_\gamma$ are strong and competitive with those obtained from gauge boson pair production at LEP II, the Tevatron and the LHC, in the case of λ_γ only weak bounds can be derived. Envisioning experimental progress concerning the measurement of the rare $K \to \pi\nu\bar{\nu}$ decays as well as theoretical advances in the calculation of the hadronic matrix elements entering ϵ'/ϵ, we have furthermore explored the potential of kaon physics to provide additional informations on the TGCs. We found that in particular ϵ'/ϵ can lead to very valuable restrictions, because Z-boson and photon contributions enter $K \to \pi\pi$ in a different way than for instance $B \to K^*\mu^+\mu^-$. In the future, this feature may help to resolve blind directions in the TGC parameter space.

Acknowledgments

We acknowledge helpful communications with Mikolaj Misiak and are grateful to him and Federico Mescia for carefully reading the manuscript and their valuable comments. We thank Joachim Brod for useful discussions and Veronica Sanz for encouraging us to write this article. We are grateful to Andrzej Buras for helpful exchange about the hadronic parameter R_8 that enters the prediction for ϵ'/ϵ, Aneesh Manohar for explanations concerning his work [30] and David Straub for providing further details on his analysis [47]. UH thanks Michael Trott for an invitation to the workshop "HEFT2014 – Higgs Effective Field Theories". He also acknowledges the hospitality and support of the CERN theory division.

References

[1] S. Schael *et al.* [ALEPH and DELPHI and L3 and OPAL and SLD and LEP Electroweak Working Group and SLD Electroweak Group and SLD Heavy Flavour Group Collaborations], Phys. Rept. **427**, 257 (2006) [hep-ex/0509008].

[2] T. Aaltonen *et al.* [CDF Collaboration], Phys. Rev. Lett. **104**, 201801 (2010) [arXiv:0912.4500 [hep-ex]].

[3] T. Aaltonen *et al.* [CDF Collaboration], Phys. Rev. D **86**, 031104 (2012) [arXiv:1202.6629 [hep-ex]].

[4] V. M. Abazov *et al.* [D0 Collaboration], Phys. Lett. B **718**, 451 (2012) [arXiv:1208.5458 [hep-ex]].

[5] S. Schael *et al.* [ALEPH and DELPHI and L3 and OPAL and LEP Electroweak Collaborations], Phys. Rept. **532**, 119 (2013) [arXiv:1302.3415 [hep-ex]].

[6] T. Corbett, O. J. P. Čboli, J. Gonzalez-Fraile and M. C. Gonzalez-Garcia, Phys. Rev. Lett. **111**, no. 1, 011801 (2013) [arXiv:1304.1151 [hep-ph]].

[7] S. Chatrchyan *et al.* [CMS Collaboration], Eur. Phys. J. C **73**, no. 10, 2610 (2013) [arXiv:1306.1126 [hep-ex]].

[8] S. Chatrchyan *et al.* [CMS Collaboration], Phys. Rev. D **89**, 092005 (2014) [arXiv:1308.6832 [hep-ex]].

[9] G. Aad *et al.* [ATLAS Collaboration], JHEP **1501**, 049 (2015) [arXiv:1410.7238 [hep-ex]].

[10] J. Ellis, V. Sanz and T. You, arXiv:1410.7703 [hep-ph].

[11] A. Falkowski and F. Riva, JHEP **1502**, 039 (2015) [arXiv:1411.0669 [hep-ph]].

[12] S. P. Chia, Phys. Lett. B **240**, 465 (1990).

[13] K. A. Peterson, Phys. Lett. B **282**, 207 (1992).

[14] K. Numata, Z. Phys. C **52**, 691 (1991).

[15] T. G. Rizzo, Phys. Lett. B **315**, 471 (1993) [hep-ph/9304263].

[16] X. G. He, Phys. Lett. B **319**, 327 (1993) [hep-ph/9306254].

[17] G. Baillie, Z. Phys. C **61**, 667 (1994) [hep-ph/9307369].

[18] S. Dawson and G. Valencia, Phys. Rev. D **49**, 2188 (1994) [hep-ph/9308248].

[19] X. G. He and B. McKellar, Phys. Lett. B **320**, 165 (1994) [hep-ph/9309228].

[20] X. G. He and B. H. J. McKellar, Phys. Rev. D **51**, 6484 (1995) [hep-ph/9405288].

[21] S. Alam, S. Dawson and R. Szalapski, Phys. Rev. D **57**, 1577 (1998) [hep-ph/9706542].

[22] G. Burdman, Phys. Rev. D **59**, 035001 (1999) [hep-ph/9806360].

[23] X. G. He, Phys. Lett. B **460**, 405 (1999) [hep-ph/9903242].

[24] J. Brod, A. Greljo, E. Stamou and P. Uttayarat, JHEP **1502**, 141 (2015) [arXiv:1408.0792 [hep-ph]].

[25] R. Röntsch and M. Schulze, JHEP **1407**, 091 (2014) [arXiv:1404.1005 [hep-ph]].

[26] K. Hagiwara, S. Ishihara, R. Szalapski and D. Zeppenfeld, Phys. Rev. D **48**, 2182 (1993).

[27] K. Hagiwara, R. D. Peccei, D. Zeppenfeld and K. Hikasa, Nucl. Phys. B **282**, 253 (1987).

[28] W. Buchmüller and D. Wyler, Nucl. Phys. B **268**, 621 (1986).

[29] B. Grzadkowski, M. Iskrzynski, M. Misiak and J. Rosiek, JHEP **1010**, 085 (2010) [arXiv:1008.4884 [hep-ph]].

[30] E. E. Jenkins, A. V. Manohar and M. Trott, JHEP **1401**, 035 (2014) [arXiv:1310.4838 [hep-ph]].

[31] A. Freitas and U. Haisch, Phys. Rev. D **77**, 093008 (2008) [arXiv:0801.4346 [hep-ph]].

[32] B. Grzadkowski and M. Misiak, Phys. Rev. D **78**, 077501 (2008) [Erratum-ibid. D **84**, 059903 (2011)] [arXiv:0802.1413 [hep-ph]].

[33] A. S. Kronfeld, R. S. Tschirhart, U. Al-Binni, W. Altmannshofer, C. Ankenbrandt, K. Babu, S. Banerjee and M. Bass *et al.*, arXiv:1306.5009 [hep-ex].

[34] U. Haisch and A. Weiler, Phys. Rev. D **76**, 074027 (2007) [arXiv:0706.2054 [hep-ph]].

[35] U. Haisch and S. Westhoff, JHEP **1108**, 088 (2011) [arXiv:1106.0529 [hep-ph]].

[36] M. Misiak, H. M. Asatrian, R. Boughezal, M. Czakon, T. Ewerth, A. Ferroglia, P. Fiedler and P. Gambino *et al.*, arXiv:1503.01789 [hep-ph].

[37] M. Czakon, P. Fiedler, T. Huber, M. Misiak, T. Schutzmeier and M. Steinhauser, arXiv:1503.01791 [hep-ph].

[38] Y. Amhis *et al.* [Heavy Flavor Averaging Group (HFAG) Collaboration], arXiv:1412.7515 [hep-ex].

[39] C. Bobeth, M. Gorbahn, T. Hermann, M. Misiak, E. Stamou and M. Steinhauser, Phys. Rev. Lett. **112**, 101801 (2014) [arXiv:1311.0903 [hep-ph]].

[40] T. Hermann, M. Misiak and M. Steinhauser, JHEP **1312**, 097 (2013) [arXiv:1311.1347 [hep-ph]].

[41] C. Bobeth, M. Gorbahn and E. Stamou, Phys. Rev. D **89**, no. 3, 034023 (2014) [arXiv:1311.1348 [hep-ph]].

[42] V. Khachatryan *et al.* [CMS and LHCb Collaborations], arXiv:1411.4413 [hep-ex].

[43] M. Ciuchini, E. Franco, S. Mishima and L. Silvestrini, JHEP **1308**, 106 (2013) [arXiv:1306.4644 [hep-ph]].

[44] D. Guadagnoli and G. Isidori, Phys. Lett. B **724**, 63 (2013) [arXiv:1302.3909 [hep-ph]].

[45] P. Gambino, U. Haisch and M. Misiak, Phys. Rev. Lett. **94**, 061803 (2005) [hep-ph/0410155].

[46] F. Beaujean, C. Bobeth and D. van Dyk, Eur. Phys. J. C **74**, no. 6, 2897 (2014) [Erratum-ibid. C **74**, no. 12, 3179 (2014)] [arXiv:1310.2478 [hep-ph]].

[47] W. Altmannshofer and D. M. Straub, arXiv:1411.3161 [hep-ph].

[48] R. Aaij *et al.* [LHCb Collaboration], Phys. Rev. Lett. **113**, no. 15, 151601 (2014) [arXiv:1406.6482 [hep-ex]].

[49] A. J. Buras, M. Gorbahn, U. Haisch and U. Nierste, Phys. Rev. Lett. **95**, 261805 (2005) [hep-ph/0508165].

[50] A. J. Buras, M. Gorbahn, U. Haisch and U. Nierste, JHEP **0611**, 002 (2006) [Erratum-ibid. **1211**, 167 (2012)] [hep-ph/0603079].

[51] J. Brod and M. Gorbahn, Phys. Rev. D **78**, 034006 (2008) [arXiv:0805.4119 [hep-ph]].

[52] J. Brod, M. Gorbahn and E. Stamou, Phys. Rev. D **83**, 034030 (2011) [arXiv:1009.0947 [hep-ph]].

[53] NA62 Collaboration, http://na62.web.cern.ch/na62

[54] KOTO Collaboration, http://koto.kek.jp

[55] ORKA Collaboration, http://projects-docdb.fnal.gov/cgi-bin/ShowDocument?docid=1365

[56] M. Bauer, S. Casagrande, U. Haisch and M. Neubert, JHEP **1009**, 017 (2010) [arXiv:0912.1625 [hep-ph]].

[57] A. J. Buras, F. De Fazio and J. Girrbach, Eur. Phys. J. C **74**, no. 7, 2950 (2014) [arXiv:1404.3824 [hep-ph]].

[58] T. Blum, P. A. Boyle, N. H. Christ, N. Garron, E. Goode, T. Izubuchi, C. Jung and C. Kelly *et al.*, Phys. Rev. D **86**, 074513 (2012) [arXiv:1206.5142 [hep-lat]].

[59] T. Blum, P. A. Boyle, N. H. Christ, J. Frison, N. Garron, T. Janowski, C. Jung and C. Kelly *et al.*, arXiv:1502.00263 [hep-lat].

[60] K. A. Olive *et al.* [Particle Data Group Collaboration], Chin. Phys. C **38**, 090001 (2014).